Available online at www.sciencedirect.com
ScienceDirect
International Journal of Pharmaceutics 343 (2007) 208–219
INTERNATIONAL JOURNAL OF PHARMACEUTICS
www.elsevier.com/locate/ijpharm

Physicochemical stability of lipid injectable emulsions: Correlating changes in large globule distributions with phase separation behavior

Thomas Gonyon, Pankaj Patel, Heather Owen, Andrew J. Dunham, Phillip W. Carter *

Technology Resources, Rt. 120 and Wilson Rd., Baxter Healthcare, Round Lake, IL 60073, United States

Received 1 April 2007; received in revised form 15 May 2007; accepted 16 May 2007
Available online 24 May 2007

Abstract

Single particle optical sensing (SPOS) and visual inspection were used to characterize a series of lipid injectable emulsions ($n = 21$) featuring three lipid types, two electrolyte conditions, and three pH levels (7.0, 4.75, and 2.5). Seven of the twenty-one sample conditions exhibited phase separation instability by visual inspection within 98 h of emulsion preparation. The phase instability was driven by electrolyte type and pH, and "cracking" phenomena were independent of lipid type despite the base lipids ranging almost two orders of magnitude in $PFAT_5$ levels. Logistic regression analysis showed that the $PFAT_5$ level determined 1 h after admixture preparation was not correlated with phase separation behavior. However, $PFAT_5$ measured at later times showed much improved correlations with emulsion instability. $PFAT_5$ was highly correlated with neighboring cumulative distributions termed $PFAT_X$ where $X = 2$–10 μm. Although the admixtures studied were not clinically relevant, the data demonstrate some limitations of developing empirical correlations between single-point SPOS measurements and emulsion instability. An alternative limit test for emulsion stability based on the rate of change in the large globule counts is proposed to mitigate inherent deficiencies in the current USP Chapter ⟨729⟩ limit test based on single-point determination of $PFAT_5$ values.

Keywords: Emulsion stability; Light obscuration; Total parenteral nutrition; Lipids

1. Introduction

Lipid emulsions have been used as key components of total nutritional admixtures (TNAs) for many years serving as an effective delivery vehicle for essential fats and energy (Brown et al., 1986). The successful application of emulsion technology relies on safely meeting nutritional needs provided by its composition while avoiding undesired side effects. One of the more significant safety concerns relates to acceptable concentration limits of larger-sized fat globules present in the TNA. Large globules (≥5 μm) that exceed the diameter of capillaries are postulated to become trapped within these vessels (Kanke et al., 1980; Illum et al., 1982). The result of such embolic occlusions is hypothesized to be tissue injury (i.e., necrosis), inflammation, and compromised organ function. Despite years of safe and effective use of TNAs, clinical concerns related to lipid globule sizes exceeding 5 μm remain and have stimulated recent interest in development of guidelines for the characterization of lipid emulsions (Muller and Heinemann, 1992). Generating appropriate guidelines with respect to lipid emulsion globule size distribution (GSD) are intended to improve the safe infusion of lipid emulsions across a variety of clinical uses.

Defining appropriate GSD requirements for lipid emulsions will at a minimum require methods or characterization techniques that reliably measure GSD attributes. To this end, the introduction of single particle optical sensing (SPOS) has had a significant, favorable impact on elucidating details of the GSD "tail" populated with the larger fat globules (Sayeed et al., 1987; Bullock et al., 1992; Mehta et al., 1992). SPOS is a technique based on light obscuration by individual globules, and while unable to accurately assess the GSD mean diameter, globule sizes greater than about 2 μm in diameter can be accurately determined. The use of Coulter counters based on electrical pulse counting have also been widely applied to characterization of the larger globules in the GSD tail (Tripp et al., 1990; Washington et al., 1993; Muller and Heinemann, 1994; Rey et al., 2005). On the other hand, traditional particle sizing techniques based on light scattering (laser diffraction and dynamic light scattering)

* Corresponding author. Tel.: +1 11 847 270 2428; fax: +1 11 847 270 5449.
E-mail address: phillip_carter@baxter.com (P.W. Carter).

0378-5173/$ – see front matter © 2007 Elsevier B.V. All rights reserved.
doi:10.1016/j.ijpharm.2007.05.038

provide useful information about the mean size of the GSD but are insensitive to changes in the GSD tail (Driscoll et al., 2001a). Microscopic methods of analysis are labor intensive and more susceptible to sampling errors. Thus, they are less likely to reflect lipid globule size distributions of samples (Harrie et al., 1986). Since the conclusions from GSD evaluation are highly method dependent (Zhang and Kirsch, 2003), characterizing the complete GSD requires at least two techniques with one technique assessing mean globule size and another method describing the fraction of larger-sized globules. Since SPOS accurately sizes globules with diameters greater than about 2 μm, it is logical to leverage this technique when evaluating relationships between large globule concentrations or changes in large globule concentrations and stability.

Driscoll et al. utilized SPOS to characterize lipid emulsions and was first to propose an upper limit of 0.40% for the percentage of fat residing in globules greater than 5 μm ($PFAT_5$) for predicting stability of total nutrient admixtures (Driscoll et al., 1995). Over the last decade, Driscoll has repeatedly asserted that lipid emulsions with starting $PFAT_5$ levels above a threshold value are unstable, and therefore are unsafe for clinical use (Driscoll et al., 1996; Driscoll, 1997; Driscoll et al., 2000; Driscoll et al., 2001a; Driscoll et al., 2001b; Driscoll et al., 2002; Driscoll et al., 2003; Driscoll, 2006). Based largely on this body of work, the U.S. Pharmacopeia (USP) has decided to adopt a proposed Chapter ⟨729⟩, "Globule Size Distribution in Lipid Injectable Emulsions" (US Pharmacopeia 30/NF 25 Supplement 2, 2007). In addition to mean globule size requirements determined by other methods, Chapter ⟨729⟩ mandates the SPOS-determined $PFAT_5$ levels of parent lipid emulsions be less than 0.05%.

For parenteral lipid emulsions, the need for an effective predictor of emulsion stability has existed for many years (Koster et al., 1996) along with the need for a clear definition of stability (Ball, 2001). However, the current USP $PFAT_5$ limit for parent lipid emulsions uses a $PFAT_5$ level proposed primarily on the basis of manufacturer capability rather than emulsion stability (Driscoll et al., 2001a). The proposed level also appears to contradict previous studies where a number of lipid emulsion admixtures that exceeded 0.05% were deemed stable (Sayeed et al., 1987; Bullock et al., 1992; Mehta et al., 1992, Driscoll et al., 1995). Therefore, it is prudent to examine the emulsion instability basis for this new USP requirement within the context of established principals of colloidal stability.

It is well known that all lipid emulsions are thermodynamically unstable systems with respect to water and oil phase separation (Sinko, 2006). TNAs belong to a class of emulsions designed, formulated, and prepared to be kinetically stable and remain suspended as submicron oil droplets in aqueous medium for long periods of time. Precisely how long these suspended droplets are stable is a function of many factors including pH, electrolytes, emulsifying agents, co-additives, and storage conditions (Washington, 1990; Brown et al., 1986). Specifying the time regime for stability is of great practical significance, and for TNAs the clinically relevant time domains are generally a maximum of 30 h at room temperature (24 h hang time) and 7 days refrigerated. The parent emulsion will have much longer specified stabilities of up to 24 months. Independent of emulsion composition, it is generally accepted that the most precise method of stability determination with respect to globule size requires a size-frequency analysis as a function of time (King and Mukherjee, 1939). The USP Chapter ⟨729⟩ does not incorporate, for any globule size determination, the rate of change in GSD, and therefore seems inherently deficient for stability prediction.

Mechanistically, many factors already mentioned above can influence the interfacial and transport properties of globules resulting in a wide variety of physicochemical phenomena such as phase separation, flocculation, creaming, globule coalescence, or even chemical hydrolysis (Heurtault et al., 2003). The interdependencies of these processes are complex. A comprehensive review of emulsion dynamics indicates that existing models are inadequate for predicting TNA stability due to unique compositions, high globule concentrations, unknown aggregate structures, and high polydispersities to name just a few mitigating variables (Dukhin et al., 2006). Clearly, the GSD time-dependent behavior has many influential factors and multiple physicochemical kinetic pathways available. In light of the challenges with a "first principles" approach, developing SPOS empirical relationships with stability is quite reasonable especially given the natural, expected progression from globule growth to phase separation. However, predicting emulsion stability exclusively from SPOS-based outputs presents challenges owing to the diversity of commercial emulsion variables and destabilization mechanisms available.

The purpose of this paper is to further evaluate SPOS as an empirical predictor of lipid emulsion stability with respect to phase separation determined by visual inspection. In the absence of sufficient data supporting alternative definitions, phase separation was chosen as the unambiguous criterion for instability. It is understood that other failure criteria for stability can likely be established prior to phase separation, but that all phase-separated emulsions are unstable. In this study, a series of three lipid emulsions with a range of $PFAT_5$ values were prepared under seven different solution conditions to monitor SPOS and phase separation behavior ($n = 21$) over 98 h. The relationship between SPOS output and phase separation behavior are explored with special attention to the uniqueness of $PFAT_5$ relative to $PFAT_X$ where $X = 2$–10 μm. Although the emulsion conditions are not of clinical significance, they are intended to sample a broader range of formulation space to capture unique failure modes. The methodology is generally applicable and evaluates the USP Chapter ⟨729⟩ approach by exploring time dependencies, phase separation, and cumulative distributions adjacent to $PFAT_5$.

2. Materials and methods

2.1. Experimental design

In this study, a 3-factor multilevel general factorial design was used to allow direct comparison of three lipid types (Table 1) fixed at test concentrations of 10 wt.% at varying pH and electrolyte conditions as described in Table 2. The three lipid types were chosen to span a range of $PFAT_5$ values as shown in

Table 1
Soybean oil lipid emulsion types used to prepare test conditions

Lipid ID	Name	$PFAT_5$ (%)[a]	Container	Expiry	lot #	Manufacturer
I_H	Intralipid	0.312	Flexible	12/07	UA10313	Fresenius Kabi
I_L	Intralipid	0.042	Flexible	04/08	UE12612	Fresenius Kabi
L3	Liposyn III	0.007	Glass	9/13/07	39–388 DE	Hospira

[a] As reported in Table 4 of this work at $t = 1.0$ h.

Table 2
3-Factor multilevel general factorial design used for generating lipid test conditions

Factor	Levels
Electrolyte type	Procalamine, Clinimix E 5/25 without dextrose, water[a]
pH	2.5, 4.75, 7.0
Lipid Type	I_H, I_L, L3 (described in Table 1)

[a] Only used in creating the three control samples.

Table 1. The $PFAT_5$ values of 0.312%, 0.042%, 0.007% in Table 1 were taken from $t = 1.0$ h of the controls in the Section 3. The electrolyte diluents (Procalamine or Clinimix E 5/25 without dextrose) and pH values (2.5, 4.75, 7.0) were chosen to span a range of lipid response conditions. The design of two electrolyte solutions, three pH values, and three lipid types produces a matrix of 18 sample conditions plus the three control solutions to produce a grand total of 21 lipid emulsion conditions. The lipid controls were made by simple 2-fold dilution of the lipid emulsion with 0.2 μm filtered, distilled water. Each lipid test condition is defined in Table 3. The order of condition preparation and testing was randomized.

The primary goal of this study design was to produce a series of test samples which exhibited a range of phase separation behavior over a storage interval of 4 days at $25 \pm 2\,^{\circ}C$. Evidence of phase separation or cracking was determined by visual inspection (see details below) at predetermined time intervals of 6.5, 25, 49, 75, and 98 h and compared to SPOS measurements recorded at time intervals of 1.0, 6.5, 25, 49, 75, and 98 h. Statistical tools (MINITAB v. 14) were used in data analysis to establish relationships between the observed stability and SPOS measurements. It is important to note that the test solutions in this design were not selected on the basis of relevance to any clinical formulation but rather were selected to produce a range of stability, with instability defined as the presence of irreversible phase separation of the emulsion within the 4-day time interval of the study.

2.2. Materials

Samples were prepared by 2-fold dilution of 20 wt.% lipid emulsion products with the appropriate electrolyte diluent. Specifically, 20 g of lipid was added to 20 g of pH-adjusted electrolyte in a 50 mL plastic centrifuge tube followed by tube inversion 20 times for complete mixing. The pH of the electrolyte was adjusted prior to lipid addition using concentrated HCl (pH 2.5), 5 N HCl (pH 4.75), or 5 N NaOH (pH 7) as appropriate, and the buffering capacity of the electrolyte solution maintained the pH throughout the duration of the experiment. The control solutions were made using filtered, distilled water as

Table 3
Lipid sample condition description with first observed evidence of cracking and translation to 98 h phase-separated criterion

Condition no.	pH	Lipid type	Electrolyte[a]	First observed cracking (h)	Phase-separated?[b]
1	2.5	I_L	Procalamine	49	Yes
2	2.5	I_L	Clinimix E 5/25	>98	No
3	2.5	I_H	Procalamine	75	Yes
4	2.5	I_H	Clinimix E 5/25	>98	No
5	2.5	L3	Procalamine	6.5	Yes
6	2.5	L3	Clinimix E 5/25	>98	No
7	4.75	I_L	Procalamine	75	Yes
8	4.75	I_L	Clinimix E 5/25	>98	No
9	4.75	I_H	Procalamine	75	Yes
10	4.75	I_H	Clinimix E 5/25	>98	No
11	4.75	L3	Procalamine	98	Yes
12	4.75	L3	Clinimix E 5/25	>98	No
13	7.0	I_L	Procalamine	98	Yes
14	7.0	I_L	Clinimix E 5/25	>98	No
15	7.0	I_H	Procalamine	>98	No
16	7.0	I_H	Clinimix E 5/25	>98	No
17	7.0	L3	Procalamine	>98	No
18	7.0	L3	Clinimix E 5/25	>98	No
C1	8.0	I_H	Distilled water	>98	No
C2	8.0	I_L	Distilled water	>98	No
C3	8.5	L3	Distilled water	>98	No

[a] Without dextrose.
[b] At observation time = 98 h.

the diluent without any pH adjustment. The pH was determined using an Orion pH meter.

Additional information regarding the Intralipid, Liposyn III, Clinimix E, and Procalamine products used in this study is available in the package inserts for each product. Briefly, Procalamine (3% amino acid and 3% glycerin injection with electrolytes), produced by B Braun Irvine Ca., is a sterile, nonpyrogenic, moderately hypertonic intravenous injection containing crystalline amino acids, a nonprotein energy substrate and maintenance electrolytes packaged in a glass bottle. Clinimix E 5/25 (amino acid with electrolytes in dextrose with calcium) injection, produced by Baxter Healthcare, Deerfield Il., is a sterile, nonpyrogenic, hypertonic solution in a Clarity Dual chamber plastic container. In this study, only the amino acid chamber which contains 10% amino acid with electrolytes of the Clinimix E 5/25 unit was used. To mimic the dilution which would normally occur when the two chambers of the clinimix E 5/25 product are mixed, the amino acid chamber was diluted 1:1 with filtered distilled water (DF-2) to produce a final amino acid concentration of 5% prior to further processing.

Each 100 mL of 20% Intralipid, produced for Baxter Healthcare, Deerfield Il by Fresenius Kabi, Uppsala Sweden, contains 20.0 g soybean oil, 1.2 g phospholipids (from powdered egg yolk) 2.25 g Glycerin USP and water for injection q.s. Each 100 mL of 20% Liposyn III, produced by Hospira, Lake Forest, Il., contains 20 g soybean oil, 1.2 g egg phosphatides added as an emulsifier, and 2.5 g glycerin.

2.3. Visual inspection

Macroscopic examination of all samples was made at all measurement intervals starting with $t = 6.5$ h by visual inspection. The examination inspected the centrifuge tubes for signs of creaming (dense white layer at the surface of a mixture) or the presence of free oil. Although centrifuge tubes were used as containment vessels, there was no sample centrifugation performed at any time. Free oil may be clear or yellow in color, which floats on the surface of the sample and cannot be dispersed by agitation. A sample was judged to be stable if it appeared to be "milky" white and opaque with a non-reflective surface and there was also no evidence of breakage or precipitation. A broken emulsion was defined as an emulsion appearing as a white, opaque mixture with a clear or amber oil layer that floated on the surface and cannot be re-dispersed by agitation.

The test samples were placed against a lighted white background and any visual observations of phase separation were recorded. All samples were photographed with a Nikon Coolpix E995 S/N 352847 digital camera after placing the samples against a lighted background. The photographs were then transferred into Adobe Photoshop version 7.0 and brightened for image enhancement of sample labels and phase behavior.

2.4. Single particle optical sensing

Droplet size analysis and distribution of each test mixture at all intervals was determined using the AccuSizer^{TM} (Model 770, Particle Sizing Systems, Santa Barbara, CA) equipped with the Pressure Assisted Liquid Sampler (PALS) and utilizing an LE 400 sensor in extinction mode previously calibrated with polystyrene latex spheres. Glass containers with magnetic stir bars were exhaustively rinsed with filtered distilled water prior to transfer of samples. The filled containers were then placed into the PALS unit and the background was assured to be below 0.01 particle/mL >2 μm prior to using the glassware for dilution. The pressure setting of the PALS system was set at 48 psi to produce a flow rate of 60 mL/min, corresponding to the calibration flow rate of the sensor.

The sample centrifuge tube was inverted 20 times and a sample aliquot was removed with a calibrated autopipette, transferred to the filled beaker, and allowed to mix for 60 s on a magnetic stirring plate. Dilution factors ranged from 500 to 32,000 to achieve an acceptable level of cumulative particle counts within the targeted range of 1000–7000 counts/mL. This concentration of particles was selected to obtain a significant signal intensity while avoiding the coincidence limit of the sensor which is approximately 9000 particles/mL. Within particle counts that avoid coincidence limits, no significant variation in normalized globule counts was observed as a function of dilution factor for representative conditions.

2.5. Particle sizing for estimating mean GSD

The Horiba LA-920 Laser Scattering Particle Size Distribution Analyzer was used in this study to examine the globule size distribution. The laser diffraction testing was performed at time intervals $t = 25$ h and $t = 98$ h. After the sample tube was inverted 20 times, the samples were analyzed using filtered distilled water as the diluent with a relative refractive index of 1.12 and an imaginary term set to 0.01. The volume-weighted mean and 99th percentiles were recorded.

2.6. pH measurements

An Orion Model 330 pH meter with a combination electrode (Thermo, Model PerPHect Electrode Glass Combination pH probe) was calibrated with either 1.68, 4.01, 6.86 or 9.18 standard buffer solutions (Radiometer Analytical S.A., France) bracketing the expected pH range of the samples and pH measurements were performed after inverting the sample 20 times. All pH measurements were found to be within 0.15 pH units of their targeted value.

2.7. Calculation of $PFAT_X$ from Accusizer data

The calculation and technique for employing a particle counter to assess the number of larger oil droplets present in a lipid emulsion has been described elsewhere (Driscoll et al., 1995). The results of the measurement are a series of particle counts at specific particle sizes. The counts were transferred from the PALS software to Microsoft Excel for calculation of $PFAT_X$, where $X = 2$–10 μm. The particle size data are normalized to report the percentage of fat in the lipid emulsion that is present as particles above a specified diameter by conversion to a volume basis.

Normalization of the data requires the conversion of results for each size channel to its equivalent spherical volume (ESV) using the following formula:

$$\mathrm{ESV(cm^3)} = \frac{(\pi \times D^3)}{6}$$

where D: diameter in centimeters and ESV: is expressed in cubic centimeters. The diameter was calculated as the geometric mean of the upper and lower boundary for each channel. Next the number of particles counted in that particular size bin is multiplied by the ESV for that size bin yielding a calculated total spherical volume (TSV) for a given channel of data.

$$\mathrm{TSV} = \text{number of particles} \times \mathrm{ESV}$$

The percentage of fat concentration of the TNA existing as enlarged lipid globules is then calculated using the following formula:

$$\%\mathrm{FAT} = \left[100 \times \frac{[\mathrm{TSV\,(cm^3)} \times \mathrm{Density\,(g/mL)} \times \mathrm{Dilution\ Factor}]}{\left[\mathrm{Sample\ Volume\,(cm^3)} \times \mathrm{Final\ Fat\ Composition\,(g/mL)}\right]}\right]$$

where the density of soybean oil was set equal to 0.92 g/mL. The PFAT_X values were calculated for particle sizes 2–10 μm.

3. Results

The emulsion stability for each lipid condition was determined by visual inspection where the appearance of a clear or yellow liquid on the surface was taken as an indication of phase separation or "cracking". Fig. 1 illustrates representative micrographs associated with lipid condition 1 where the first visual observation of cracking occurred at $t = 49$ h. At early times, $t = 6.5$ h, the lipid emulsion is completely homogeneous in appearance. Some white, particulate inhomogeneities are observed at $t = 25$ h on the containment vessel surface for condition 1 indicating some large agglomerate formation or precipitate. At $t = 49$ h there is a yellow liquid observed at the air–liquid interface which is a positive indication for cracking. By $t = 75$ h, the emerging oil has formed a significant layer about 2 mm thick on top of the aqueous phase. This progression of observations is typical for most emulsion conditions that were positive for cracking (phase separation). Stable emulsions remained identical in appearance (for 98 h) to their appearance at $t = 6.5$ h showing no significant visual inhomogeneities.

Table 3 summarizes the visual inspection results by recording the time of the first visual observation of an oil layer or large droplet (>2 mm diameter). The table shows that lipid condition 5 (lipid L3/Procalamine/pH 2.5) was the first to crack with clear separation observed by $t = 6.5$ h, and this represents the most unstable lipid condition in the experimental design. In contrast to condition 5, all the even-numbered conditions (prepared with the Clinimix E electrolyte) and the control conditions (filtered distilled water) did not exhibit any signs of cracking within the 98 h observation window, and therefore were considered stable within the experimental timeframe. The odd-numbered conditions 1–13 (prepared with the Procalamine electrolyte) all displayed cracking within 98 h. Other visual observations included white particulates accumulating near the emulsion air/liquid interface and on the containment vessel as mentioned above. Often a "ring" of white or yellow was also observed just above the emulsion surface on the containment vessel of unstable conditions.

Since the central purpose of this study is the evaluation of relationships between lipid emulsion phase separation behavior and the SPOS measurements, establishing reliable, measurable

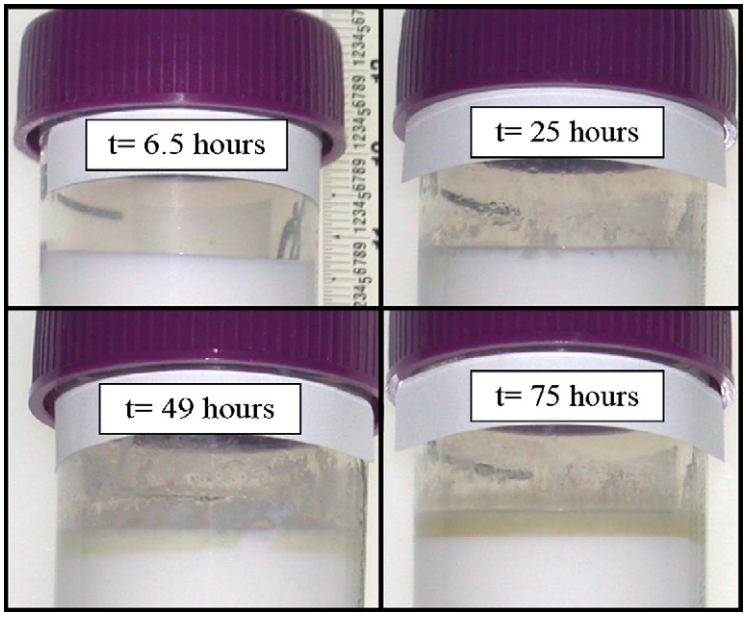

Fig. 1. Photographs of condition 1 taken at four different storage times representative of visual observations of homogeneous emulsion (6.5 h), some particulate formation (25 h), first evidence of cracking (49 h), and complete layer of phase-separated oil (75 h).

phase separation criteria is essential. Due to the qualitative nature of visual inspection methods combined with limited time-dependent observations per condition ($n = 6$), the cracking observations were transformed to a binary output at $t = 98$ h as indicated in Table 3. While the kinetic aspects of phase separation phenomena are important, the quantitative scope of this study is directed toward modeling cracking instability arising within a 98 h frame. The shape of $PFAT_X$ versus time is evaluated further in Section 4.

The raw 512 channel SPOS data was converted into 1-μm channels ranging from 2 to 11 μm for ease of subsequent data analysis. The selection of 1-μm channels for analysis represents a balance between high resolution, accuracy of bin size assignments, and ease of data analysis. The time-dependent behavior of simple 2-fold dilutions of lipids I_H, I_L, and L3 in deionized water is shown in Fig. 2. These samples represent the controls C1, C2, and C3, respectively as denoted in Table 3 above. The *y*-axis is the log percentage of fat emulsion in the suspension with particle sizes greater than the sizes mapped on the *x*-axis. In other words, Fig. 2 plots the volume-weighted cumulative distribution normalized for the total lipid content in the suspension as described in Section 2.7. The term $PFAT_X$ will be used to designate the percentage of fat emulsion in the suspension with particle sizes greater than *X*. The data shows that I_H, I_L, and L3 distributions are essentially unchanged over the 98 h measurement timeframe. The absence of change in the cumulative distributions of these emulsions is consistent with an expectation of emulsion stability with simple 2-fold dilution with water. This result is consistent with the visual observations of stability described above where no evidence of cracking was observed in the control samples.

Fig. 2 also highlights the significant differences in absolute values of $PFAT_X$ for the three lipids selected for this study. The initial $PFAT_X$ values span nearly two orders of magnitude between the three lipids with values trending as follows: I_H (0.312%)> I_L (0.042%) >L3 (0.007%). The large filled circle in Fig. 2 highlights the recently adopted USP limit for $PFAT_5$ of 0.05 wt.%, and emphasizes the experimentally designed disparity between initial lipid $PFAT_5$ values. I_H-based conditions should start clearly above the adopted limit, I_L-based lipids should start near the limit, and L3-based lipids should start below this limit. Thus, the time dependence of $PFAT_5$ for the control I_H (condition C1) indicates that emulsions exceeding $PFAT_5$ values of 0.05 wt.% can be stable within the 98 h timeframe.

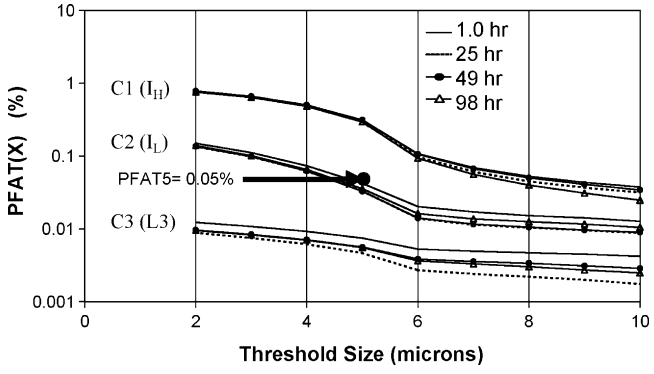

Fig. 2. $PFAT_X$ vs. *X* (where $X = 2$–10 μm) is shown for different storage times at 25 °C for the controls where a large filled circle represents the USP Chapter ⟨729⟩ $PFAT_5$ limit of 0.05%. The controls span almost two orders of magnitude in $PFAT_X$ and do not change significantly over time.

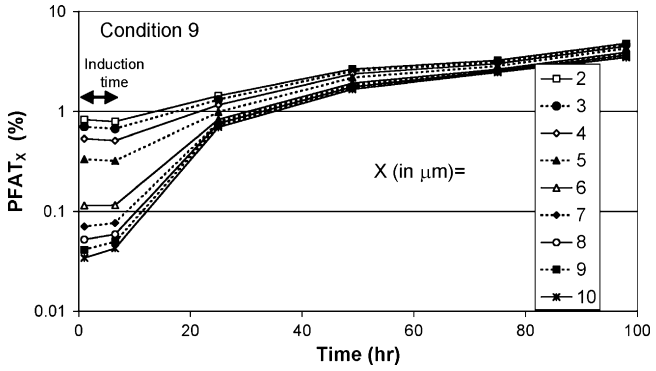

Fig. 3. $PFAT_X$ vs. time where *X* values of 2–10 μm are plotted for sample condition 9. This condition had an induction time of at least 6.5 h prior to particle growth, and similar trends were observed in the time dependence for each value of *X*.

The time dependence of $PFAT_X$ is plotted for $X = 2$–10 μm for sample condition 9 in Fig. 3. In contrast to the control samples, the $PFAT_X$ values for condition 9 increased over time following a short induction time. The induction time is simply defined here as the time before measurable changes are observed in the SPOS data, and therefore, condition 9 would have an induction time between 6.5 and 25 h. The similarity in trends for each $PFAT_X$ for values between 2 and 10 observed for condition 9 was also observed for other samples. In fact, the Pearson correlation coefficients for all the time-dependent data including the controls were greater than 0.99 with *p*-values less than 0.001 demonstrating the high degree of correlation between different $PFAT_X$ values when *X* is between 2 and 10 μm. A linear correlation between the two "bookends" of the $PFAT_X$ output is depicted graphically in Fig. 4 between $PFAT_2$ and $PFAT_{10}$. The results indicate that $PFAT_5$ is not a unique variable compared to the other $PFAT_X$ values within the range 2–10 μm, and this is not too surprising given the incremental differences associated with each step of the $PFAT_X$ cumulative distribution function.

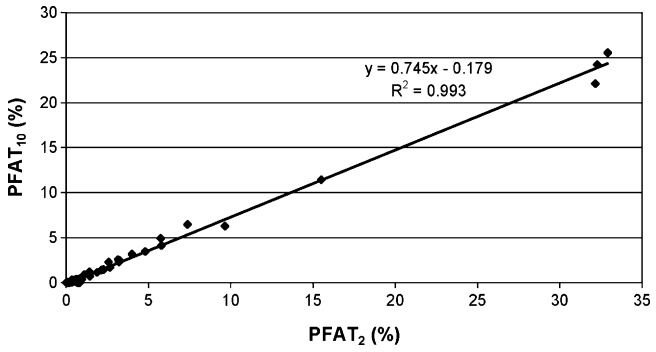

Fig. 4. A plot of $PFAT_{10}$ vs. $PFAT_2$ shows the significant correlation between the two values for all the data collected, 21 conditions measured at six different times ($n = 126$).

Table 4
$PFAT_X$ values based on SPOS measurements for $X = 2$, 5, and 10 μm

Condition	$t = 1.0$ h			$t = 6.5$ h			$t = 25$ h			$t = 49$ h			$t = 75$ h			$t = 98$ h		
	2	5	10	2	5	10	2	5	10	2	5	10	2	5	10	2	5	10
1	0.186	0.071	0.026	0.203	0.106	0.026	0.508	0.420	0.302	3.150	2.974	2.578	32.28	29.64	24.22	5.790	5.311	4.129
2	0.121	0.035	0.015	0.138	0.038	0.012	0.136	0.035	0.008	0.133	0.033	0.006	0.145	0.042	0.010	0.192	0.066	0.023
3	0.766	0.336	0.034	0.642	0.292	0.053	0.498	0.267	0.150	0.430	0.248	0.162	0.348	0.150	0.053	0.376	0.215	0.108
4	0.813	0.312	0.026	0.693	0.260	0.024	0.709	0.273	0.027	0.694	0.269	0.024	0.728	0.289	0.034	0.776	0.313	0.033
5	0.266	0.188	0.137	0.848	0.638	0.469	9.65	8.71	6.30	15.51	14.42	11.44	32.16	29.24	22.11	32.92	30.85	25.54
6	0.056	0.042	0.026	0.043	0.026	0.010	0.047	0.021	0.007	0.037	0.023	0.013	0.042	0.024	0.012	0.021	0.012	0.005
7	0.179	0.053	0.010	0.172	0.049	0.011	2.146	1.934	1.405	3.991	3.663	3.185	5.743	5.425	4.918	7.373	7.039	6.454
8	0.165	0.045	0.009	0.165	0.045	0.010	0.190	0.059	0.013	0.186	0.057	0.015	0.179	0.052	0.012	0.258	0.113	0.058
9	0.827	0.332	0.034	0.792	0.319	0.043	1.436	0.990	0.694	2.655	2.181	1.671	3.256	2.849	2.462	4.803	4.274	3.470
10	0.792	0.307	0.031	0.722	0.271	0.021	0.766	0.294	0.026	0.778	0.299	0.019	0.769	0.287	0.024	0.797	0.315	0.039
11	0.078	0.061	0.040	0.338	0.322	0.308	0.432	0.385	0.287	0.590	0.524	0.359	0.671	0.560	0.359	0.939	0.703	0.362
12	0.061	0.044	0.026	0.067	0.045	0.023	0.072	0.046	0.025	0.056	0.034	0.017	0.043	0.029	0.017	0.066	0.043	0.024
13	0.154	0.041	0.011	0.163	0.047	0.011	0.135	0.029	0.004	1.097	0.984	0.914	1.415	1.307	1.211	2.571	2.440	2.286
14	0.147	0.041	0.012	0.145	0.038	0.010	0.142	0.034	0.006	0.202	0.073	0.037	0.143	0.039	0.009	0.150	0.040	0.012
15	0.763	0.298	0.031	0.704	0.261	0.023	0.777	0.330	0.073	1.869	1.408	1.128	2.268	1.793	1.438	3.220	2.734	2.306
16	0.741	0.299	0.040	0.707	0.263	0.021	0.705	0.264	0.028	0.794	0.320	0.037	0.731	0.279	0.022	0.757	0.294	0.026
17	0.009	0.005	0.002	0.010	0.006	0.003	0.007	0.004	0.001	0.009	0.005	0.003	0.012	0.008	0.003	0.030	0.019	0.008
18	0.012	0.007	0.004	0.009	0.005	0.002	0.009	0.005	0.002	0.011	0.007	0.004	0.009	0.006	0.003	0.008	0.004	0.002
C1	0.778	0.312	0.038	0.765	0.302	0.025	0.763	0.297	0.032	0.782	0.312	0.034	0.778	0.309	0.034	0.756	0.295	0.025
C2	0.150	0.042	0.013	0.141	0.039	0.012	0.136	0.033	0.009	0.136	0.033	0.009	0.155	0.051	0.022	0.139	0.036	0.010
C3	0.012	0.007	0.004	0.012	0.008	0.005	0.009	0.005	0.002	0.010	0.006	0.003	0.009	0.005	0.002	0.010	0.006	0.002

Due to the high degree of correlation between $PFAT_X$ values, only the $PFAT_X$ data for $X = 2$, 5, and 10 are summarized for all measurement times of 1.0, 6.5, 25, 49, 75, and 98 h in Table 4. Briefly, the data showed the even-numbered conditions, where Clinimix E is the electrolyte diluent, to have minimal changes in $PFAT_X$ as a function of time. The odd-numbered conditions (Procalamine used as the electrolyte) had more varied responses with some dramatic increases observed at longer times. Condition 5 possessed the largest increase in $PFAT_X$ levels within the first 25 h period. Initial SPOS results seem consistent with most of the visual observations documented in Table 3. A more detailed analysis of the data including correlations is presented in Section 4.

Laser diffraction measurements were made at sample times $t = 25$ h and $t = 98$ h and are depicted in Table 5. In contrast to the SPOS results, only conditions 1 and 5 show large changes in their mean and 99% particle size values at $t = 98$ h when compared to the appropriate lipid control C2 and C3, respectively. In fact, condition 5 which cracked by $t = 6.5$ h, showed a large increase in particle size by $t = 25$ h as expected based on its dramatic change in SPOS. Particle sizing by laser diffraction is just not as sensitive to changes in particle size distributions as SPOS especially in the 1–10 μm window as has been observed previously (Driscoll et al., 2001a). Conditions 7, 9, 11, 13, and 15 have significant increases in their $PFAT_X$ with only sample 9 showing any practically significant increase in its particle size characteristics determined by laser diffraction. Laser diffraction, as an ensemble average technique, is limited in its ability to measure changes to the large tail of a PSD, and therefore is not considered a useful characterization tool for establishing relationships between lipid particle/aggregate growth and phase separation behavior.

Table 5
Lipid particle size characteristics determined by laser diffraction (in microns)

Condition	$t = 25$ h		$t = 98$ h	
	Mean	99%	Mean	99%
1	0.3800	0.734	3.0700	23.828
2	0.3846	0.755	0.3708	0.683
3	0.3742	0.740	0.3685	0.725
4	0.3827	0.803	0.3722	0.744
5	6.5959	36.868	11.0398	54.506
6	0.2586	0.586	0.2554	0.576
7	0.3665	0.693	0.3672	0.710
8	0.3272	0.717	0.3247	0.718
9	0.3757	0.800	0.3911	1.190
10	0.3806	0.786	0.3736	0.784
11	0.2705	0.629	0.2803	0.657
12	0.2518	0.573	0.2392	0.581
13	0.3520	0.671	0.3245	0.662
14	0.3610	0.653	0.3625	0.654
15	0.3838	0.800	0.3738	0.767
16	0.3770	0.756	0.3711	0.756
17	0.2755	0.627	0.2523	0.576
18	0.2573	0.540	0.2457	0.564
C1	0.3762	0.785	0.3750	0.778
C2	0.3469	0.704	0.3391	0.667
C3	0.2497	0.563	0.2372	0.549

Table 6
Calculated p-values from general linear regression analysis of 98 h phase separation results

	Factors	p-value
Model 1 (R-squared (adj) = 77.92%)	pH	0.111
	Lipid type	0.444
	Electrolyte type	0.002
	pH*lipid type	0.500
	pH*electrolyte type	0.111
	Lipid type*electrolyte type	0.444
Model 2 (R-squared (adj) = 77.92%)	pH	0.047
	Electrolyte type	0.000
	pH*electrolyte type	0.047

4. Discussion

Initial statistical analysis was performed using a general linear regression model to fit the $t = 98$ h stability data as a binary response (0 = no cracking, 1 = cracking) with the experimental design factors ($n = 18$) of pH, lipid type, electrolyte type, with all interaction terms. The analysis showed only three terms of potential significance (p-values < 0.15) with the remaining terms clearly not significant (Model 1, Table 6). Removing those terms that were not significant (p-value > 0.4), resulted in electrolyte type, pH, and electrolyte*pH interaction terms as significant with p-values < 0.05 (Model 2, Table 6). The data clearly showed that the lipid type was not a significant factor contributing to lipid instability. The R^2 value of 0.78 indicates that 78% of the variation in the data is explained by just the three terms used in Model 2. Despite the broad, intrinsic variation in $PFAT_5$ incorporated into the study design by lipid type, there is no influence of lipid type on emulsion stability. Therefore, under these solution conditions, base emulsion $PFAT_5$ levels did not influence phase separation behavior. Furthermore, condition 5 prepared with the L3 base lipid possessing the lowest $PFAT_5$, was the first to phase separate. If high $PFAT_5$ were a key predictor of stability, the other two lipid conditions (1 and 3) prepared with this identical formulation (Procalamine, pH 2.5) might have been predicted to crack prior to condition 5.

The electrolyte type and pH dependence likely stems from their influence on globule surface charge. Comparing the additive contents of electrolyte and control solutions, some of the key disparities between solution compositions (Table 7) include amino acids, phosphate, calcium, and glycerin levels. Most significantly, the divalent calcium cation (present only in Procalamine) is well established as a destabilizing factor due to its influence on reducing globule surface charge (Black and Popovich, 1981; Burnham et al., 1983; Whateley et al., 1984; du Plessis et al., 1987; Washington et al., 1989). Thus, calcium-rich Procalamine is hypothesized to reduce the electrostatic stabilization between globules resulting in globule aggregation and subsequent phase separation. Similarly, conditions with lower pH values result in protonation of surface acid functionalities like phosphonates of lipid head groups reducing electrostatic stabilization resulting in globule aggregation and phase separation (Washington, 1996). Elucidating the precise mechanisms producing the observed phase separation is beyond the scope of

Table 7
Comparing additive contents of electrolyte and control solutions

Material	Test articles with Procalamine	Test articles with Clinimix E 5/25 without dextrose	Control articles
Amino acids (g/100 mL)	1.5	2.5	0
Calcium (mEq/L)	1.5	0	0
Phosphate (mmol/L)	3.5	7.5	0
Glycerin (g/100 mL)[a]	~2.7	~1.2	~1.2

[a] 10% lipid dependent variation.

the current paper, but electrostatic destabilization likely plays a significant role. The calcium-containing Procalamine and protonating power of lower pH appear to be driving emulsion instability.

Returning to the empirical analysis of SPOS output, phase separation behavior of Table 5 was examined by binary logistical regression using the logit function where each $PFAT_X$ column ($X = 2$, 5, and 10 μm) was examined as a single predictor for stability at $t = 98$ h. The regression output is summarized in Table 8 with regression coefficient p-values and Goodman–Kruskal gammas. The regression coefficient p-values need to be less than 0.05 for sufficient evidence that the coefficients are not zero using an α-level of 0.05 (95% confidence level). Goodman–Kruskal's gamma measures the degree of association between $PFAT_X$ and stability based on the difference between concordant and disconcordant pairs. Gamma lies between 0 and 1 where larger values indicate that the model has a better predictive ability. The Pearson's goodness-of-fit test for the logit function model had p-values ranging from 0.143 to 0.690 indicating that the model is a reasonable fit.

The initial measurement at $t = 1.0$ h showed the regression coefficient p-values to be much greater than 0.05 meaning there is no correlation between $PFAT_2$, $PFAT_5$, or $PFAT_{10}$ and emulsion phase separation instability at $t = 98$ h. Therefore, the level of $PFAT_X$ with $X = 2$–10 μm measured at $t = 1.0$ h is not a useful predictor of emulsion phase separation stability. The Goodman–Kruskal's low gamma values (<0.5) support this finding. The lack of relationship between $PFAT_5$ and emulsion phase separation is illustrated in Fig. 5 where the USP limit of 0.05% would have produced five false positives and one false negative for phase separation stability when examining all twenty-one conditions.

Table 8
p-values (and Goodman–Kruskal Gamma) of logistic regressions to determine association between $PFAT_X$ and cracking

Time (h)	$PFAT_2$	$PFAT_5$	$PFAT_{10}$
1	0.916 (0.27)	0.699 (0.45)	0.268 (0.42)
6.5	0.339 (0.47)	0.116 (0.69)	0.099 (0.69)
25	0.117 (0.51)	0.097 (0.71)	0.108 (0.77)
49	0.057 (0.77)	0.072 (0.84)	0.061 (0.92)
75	0.103 (0.77)	0.097 (0.84)	0.092 (0.92)
98	0.051 (0.82)	0.051 (0.84)	0.043 (0.92)

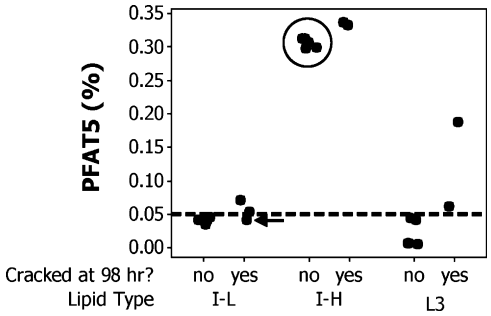

Fig. 5. Observed $PFAT_5$ values are separated by lipid type and phase separation stability. The dashed line represents the USP Chapter ⟨729⟩ limit value of 0.05% with grouping of false positives circled, and an arrow pointing to the one false negative.

At $t = 6.5$ h the regression coefficient p-values for $PFAT_5$ and $PFAT_{10}$ are significantly lower (~0.10–0.12) indicating much higher probability of nonzero coefficients but still outside of the 95% confidence limits. The $PFAT_2$ regression coefficient p-values remained high at 0.339 for the $t = 6.5$ h data point. By $t = 25$ h, p-values for $PFAT_2$, $PFAT_5$, and $PFAT_{10}$ are all between 0.097 and 0.0117. At $t = 49$ h, the regression coefficient p-values are close to 0.05 with gammas between 0.77 and 0.92. The 98 h measurement has lower p-values still. This is easily understood by recognizing that $PFAT_X$ rises well above its initial value with longer times for the unstable emulsions. Although the initial $PFAT_X$ level appears insignificant, its rate of change appears more strongly correlated with phase separation instability.

Due to the prominence of $PFAT_5$ in USP Chapter ⟨729⟩, a closer look at $PFAT_5$ trends is presented. For clarity, the $PFAT_5$ data has been partitioned according to base lipids I_H, I_L, and L3 and plotted in Figs. 6–8, respectively. While all the I_H-containing emulsions start out with $PFAT_5$ values above the adopted limit of 0.05%, 4 of the 6 samples remain stable with respect to phase separation at $t = 98$ h. In fact, all the even-numbered, Clinimix-containing I_H conditions along with the control, C1, show constant $PFAT_5$ levels (above the USP limit) with no visual evidence of cracking instability observed. A constant $PFAT_5$ level is observed for all the even-numbered, Clinimix-containing

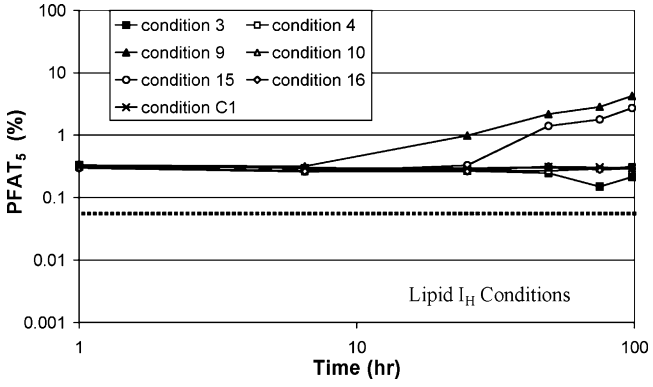

Fig. 6. Observed $PFAT_5$ values are plotted as a function of time for emulsion conditions derived from lipid I_H. The filled symbols represent phase-separated emulsions at $t = 98$ h, and the dashed line corresponds to the USP Chapter ⟨729⟩ $PFAT_5$ limit of 0.05%. While all seven conditions have $PFAT_5$ values above 0.05%, only two of the seven conditions were unstable.

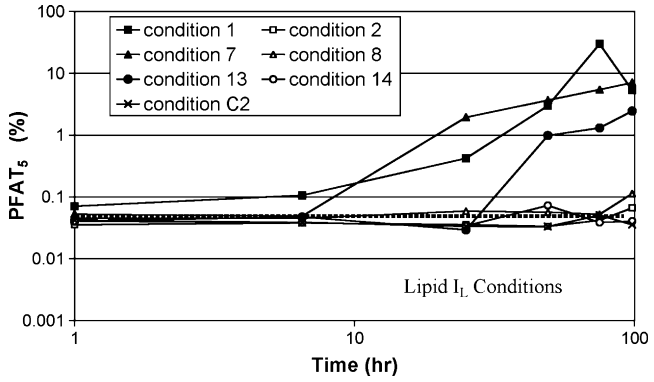

Fig. 7. Observed $PFAT_5$ values are plotted as a function of time for emulsion conditions derived from lipid I_L. The filled symbols represent phase-separated emulsions at $t = 98$ h, and the dashed line corresponds to the USP Chapter ⟨729⟩ $PFAT_5$ limit of 0.05%. Condition 13 was unstable despite an initial $PFAT_5$ value below 0.05%.

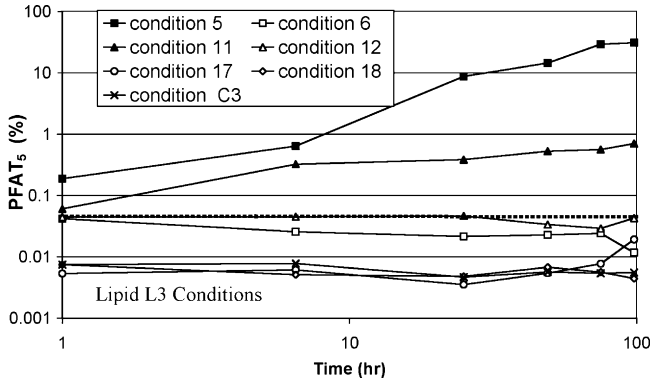

Fig. 8. Observed $PFAT_5$ values are plotted as a function of time for emulsion conditions derived from lipid L3. The filled symbols represent phase-separated emulsions at $t = 98$ h, and the dashed line corresponds to the USP Chapter ⟨729⟩ $PFAT_5$ limit of 0.05%. The $PFAT_5$ limit of 0.05% reasonably differentiates emulsion stability for emulsions derived from lipid L3.

conditions and associated controls regardless of the base lipid (I_H, I_L, or L3) comprising the emulsion. Applying the $PFAT_5$ limit of 0.05% to predict instability for I_H- and I_L-based emulsions would have resulted in 5 false positives and 1 false negative out of the 14 lipid emulsion conditions. Clearly, $PFAT_5$ is not a predictive measure of lipid emulsion stability for this group of emulsions.

The interpretation of $PFAT_5$ data changes when considering data only from L3-based lipid emulsions (Fig. 8). The $PFAT_5$ limit of 0.05% successfully predicts the relative stability in 7 out of 7 sample conditions for emulsions derived from the L3-lipid. This makes sense based on the initial levels of $PFAT_5$ at $t = 1$ h for these emulsions (Table 1). Since the starting $PFAT_5$ of the L3-based emulsions is significantly lower than 0.05%, $PFAT_5$ values exceeding the 0.05% level represents dramatic globule growth for that particular emulsion. Thus, it is the rate of increase in $PFAT_5$ that is more predictive of lipid emulsion stability than a single measurement made without context to a prior $PFAT_5$ state. In this regard, a percent increase in $PFAT_5$ or $PFAT_X$ (equivalent as discussed above) over a specified time period should be a more useful limit test for stability.

To explore a time-dependent correlation more fully, the ratio of $PFAT_5$ and $PFAT_{10}$ values at 25 h compared to 1 h is shown in Fig. 9 where values greater than one represent an increase in the $PFAT_X$ value with time. Using an arbitrary criterion of a 3-fold increase in $PFAT_{10}$ for stability, one would have effectively predicted the phase separation behavior for 20 of the 21 samples. Only condition 13 would have been missed with a false negative for instability. Interestingly, using this same criterion $PFAT_5$ would have missed conditions 3, 9, and 13 as false negatives. Sample 3 is really a differentiating condition where the globule count greater than 10 μm had a 4-fold increase compared to no increase in the globule count greater than 5 μm. Due to the very low initial counts greater than 10 μm, $PFAT_{10}$ may more accurately discriminate small changes in large globule sizes. It is noted that small decreases in $PFAT_X$ is probably due to particle adhesion and loss to the containment vessel near the surface of the emulsion. Nontheless, a ratio of $PFAT_{10}$ values taken at 2 times (1 and 25 h) has given a clear measure of globule growth that is highly correlated to phase separation instability. Even with this improvement in methodology for stability determination,

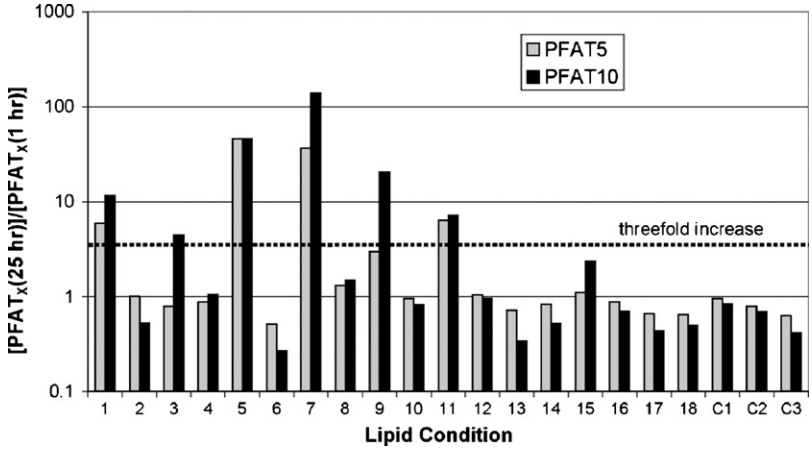

Fig. 9. The ratio of $PFAT_{10}$ ($t = 25$ h) to $PFAT_{10}$ ($t = 1$ h) is plotted for each emulsion condition along side the analogous $PFAT_5$ ratio. An arbitrary assignment of a 3-fold increase in $PFAT_{10}$ would successfully partition conditions according to their observed phase-separation behavior with the exception of condition 13. Conditions exceeding the 3-fold increase in $PFAT_{10}$ were phase-separated by $t = 98$ h.

some challenges have emerged in correlating SPOS output to phase instability.

Most significantly, the presence of an induction period prior to SPOS observable changes was detected for 3 out of the 7 conditions deemed unstable. Processes such as molecular adsorption, chemical reactions, and submicron particle formation and growth are "hidden" from SPOS measurements. At later times, the consequences of these physicochemical processes can have a significant impact on aggregation and cracking phenomena. In fact, condition 3 displayed no significant increase in $PFAT_5$, but cracking was observed by 98 h. While atypical behavior, it is another example of where empirical assignments based solely on particle size measurements may be insufficient. The observed induction phenomena are not well understood and highly variable, but represent a significant challenge to predicting instability from changes in large globule distributions.

Another challenge to predicting phase separation instability is represented by condition 15 which showed significant particle growth at $t = 25$ and 49 h without cracking by $t = 98$ h. Similarly, condition 6 and 12 showed much higher $PFAT_5$ values compared to their controls indicating some initial aggregation behavior prior to the $t = 1.0$ h measurement. These lipid emulsions showed no further increase in $PFAT_X$ or evidence of cracking, and thus, aggregated emulsion droplets do not always lead to phase separation. Interestingly, conditions 6 and 12 would still be considered stable under the current USP $PFAT_5$ limit of 0.05% despite the increase in large globules when compared to their parent globule size distributions.

Finally, SPOS is unable to distinguish between the composition or type of aggregates that lead to instability, and those which may be easily re-dispersed into the emulsion or do not impact stability. Indeed, field flow fractionation results have already demonstrated significant compositional heterogeneity of parenteral lipid emulsions that light obscuration methods would miss (Li and Caldwell, 1994; Venkatesh et al., 1998). Alternatively, there may be mechanisms of phase separation that do not require globule growth that are catalyzed at the air–liquid interface, for example. Other physical bases for instabilities preferentially associated with large globules include enhanced sedimentation (creaming), reduced specific surface area, or radius of curvature-related reactivity. It is not clear that a small percentage of large globules should have a significant impact on bulk emulsion instability from a mechanistic viewpoint.

5. Conclusions

Since fundamentals of lipid emulsion instability are still not fully understood, empirical relationships between lipid characterization measurements and phase separation remain important. The use of SPOS was found to be an effective means for monitoring the time-dependent globule growth behavior of lipid emulsions as has been reported previously. Seven of twenty-one sample conditions exhibited phase separation instability by visual inspection within 98 h of emulsion preparation. The phase instability behavior was not correlated to $PFAT_5$ values measured 1 h after sample preparation. Defining stability per USP Chapter ⟨729⟩ as a $PFAT_5$ limit value not to exceed 0.05% would have incorrectly predicted the 98 h phase separation result in 6 out of 21 samples for measurements made 1 h after sample preparation. At longer times the correlation between $PFAT_X$ and stability is much improved due to the dramatic increase in $PFAT_X$ values for phase separating conditions compared to their initial values.

As an alternative to $PFAT_5$, using a ratio of $PFAT_{10}$ (25 h)/$PFAT_{10}$ (1 h) could empirically predict phase separation stability in 20 out of 21 conditions owing primarily to $PFAT_{10}$ being more sensitive to increases in globule size compared to $PFAT_5$. The USP Chapter ⟨729⟩ $PFAT_5$ limit definition currently based on instability arguments suffers from not being defined on the basis of a measured rate of change in large fat globules. Even SPOS-based measurements that do incorporate a time-dependence in modeling instability need to be concerned with induction phenomena and phase separation mechanisms not requiring globule growth. Even though the clinical significance of the formulations in this study is limited, the breadth of destabilization pathways demonstrated underscores the challenges of an empirical approach. Further investigations are underway to develop a more robust understanding of emulsion instability with SPOS remaining as a key characterization tool.

Acknowledgements

The authors thank Dr. Gary Zaloga and Dr. Edward Chess of Baxter Healthcare for helpful discussions and review of the manuscript, and Dr. Wayne Taylor of Taylor Enterprises for review of the statistical analysis. We also thank Omayra Martinez and Syed Ameer for assistance with data acquisition.

References

Ball, P.A., 2001. Methods of assessing stability of parenteral nutrition regimens. Curr. Opin. Nutr. Metab. Care 4, 345–349.

Black, C.D., Popovich, N.G., 1981. A study of intraveneous emulsion compatibility: effects of dextrose, amino acids, and selected electrolytes. Intell. Clin. Pharm. 15, 184–193.

Brown, R., Quercia, R.A., Sigman, R., 1986. Total nutrient admixture: a review. JPEN 10, 650–658.

Bullock, L., Fitzgerald, J.F., Walter, W.V., 1992. Emulsion stability in total nutrient admixtures containing a pediatric amino acid formulation. JPEN 16, 64–68.

Burnham, W.R., Hansrani, P.K., Knott, C.E., Cook, J.A., Davis, S.S., 1983. Stability of a fat emulsion based on intraveneous feeding mixture. Int. J. Pharm. 13, 9–22.

Driscoll, D.F., Bhargava, H.N., Li, L., Zaim, R.H., Babayan, V.K., Bistrian, B.R., 1995. Physicochemical stability of total nutrient admixtures. Am. J. Health-Sys. Pharm. 52, 623–634.

Driscoll, D.F., Bacon, M.N., Bistrian, B.R., 1996. Effects of in-line filtration on lipid particle size distribution in total nutrient admixtures. JPEN 20, 296–301.

Driscoll, D.F., 1997. Physicochemical assessment of total nutrient admixture stability and safety: quantifying the risk. Nutrition 13, 166–167.

Driscoll, D.F., Bacon, M.N., Bistrian, B.R., 2000. Physicochemical stability of two types of intraveneous lipid emulsion as total nutrient admixtures. JPEN 24, 15–22.

Driscoll, D.F., Etzler, F., Barber, T.A., et al., 2001a. Physicochemical assessments of parenteral lipid emulsions:light obscuration versus laser diffraction. Int. J. Pharm. 219, 21–37.

Driscoll, D.F., Giampietro, K., Wichelhaus, D.P., et al., 2001b. Physicochemical stability assessments of lipid emulsions of varying oil composition. Clin. Nutr. 20, 151–157.

Driscoll, D.F., Nehne, J., Peterss, H., et al., 2002. The influence of medium-chain triglycerides on the stability of all-in-one formulations. Int. J. Pharm. 240, 1–10.

Driscoll, D.F., Nehne, J., Peterss, H., et al., 2003. Physicochemical stability of intravenous lipid emulsions as all-in-one admixtures intended for the very young. Clin. Nutr. 22, 489–495.

Driscoll, D.F., 2006. Lipid injectable emulsions: pharmacopeial and safety issues. Pharma. Res. 23, 1959–1969.

du Plessis, J., Van Wyk, C.J., Ackermann, C., 1987. The stability of parenteral fat emulsions in nutrition mixtures. J. Clin. Pharm. Ther. 12, 307–318.

Dukhin, S.S., Sjoblom, J., Saether, O., 2006. An experimental and theoretical approach to the dynamic behavior of emulsions. Surf. Sci. Ser.: Emulsions and Emulsion Stability 132, 1–106.

Harrie, K.R., Jacob, M., McCormick, D., Reid, J.S., McIntosh, N.L., 1986. Comparison of total nutrient admixture stability using two intraveneous fat emulsions, soyacal and intralipid 20%. JPEN 10, 381–387.

Heurtault, B., Saulnier, P., Pech, B., Proust, J.-E., Benoit, J.-P., 2003. Physicochemical stability of colloidal lipid particles. Biomaterials 24, 4283–4300.

Illum, L., Davis, S.S., Wilson, C.G., Frier, M., Hardy, J.G., Thomas, N.W., 1982. Blood clearance and organ deposition of intraveneously administered colloidal particles; the effects of particle size, nature, and shape. Int. J. Pharm. 12, 135–146.

Kanke, M., Simmons, G.Y., Weiss, D.L., Bivins, B.A., DeLuca, P.P., 1980. Clearance of 141Ce-labeled microspheres from blood and distribution in specific organs following intraveneous and intraarterial administration in beagle dogs. J. Pharm. Sci. 69, 755–762.

King, A., Mukherjee, L.N., 1939. J. Soc. Chem. Ind. 58, 243T.

Koster, V.S., Kuks, P.F.M., Lange, R., Talsma, H., 1996. Particle size in parenteral fat emulsions, what are the true limitations? Int. J. Pharm. 134, 235–238.

Li, J., Caldwell, K.D., 1994. Structural studies of commercial fat emulsions used in parenteral nutrition. J. Pharm. Sci. 83, 1586–1592.

Mehta, R.C., Head, L.F., Hazrati, A.M., Parr, M., Rapp, R.P., Deluca, P.P., 1992. Fat emulsion particle-size distribution in total nutrient admixtures. Am. J. Hosp. Pharm. 49, 2749–2755.

Muller, R.H., Heinemann, S., 1992. Fat emulsions for parenteral nutrition. I. Evaluation of microscopic and laser light scattering methods for the determination of the physical stability. Clin. Nutr. 11, 223–236.

Muller, R.H., Heinemann, S., 1994. Fat emulsions for parenteral nutrition. IV. Lipofundin MCT/LCT regimens for the total parenteral nutrition (TPN) with high electrolyte load. Int. J. Pharm. 107, 121–132.

Rey, J.B., Faure, C., Brion, F., 2005. Stability of all-in-one standard formulae for paediatric parenteral nutrition. PDA J. Pharm. Sci. Technol. 59, 206–220.

Sayeed, F.A., Tripp, M.G., Sukumaran, K.B., et al., 1987. Stability of total nutrient admixtures using various intraveneous fat emulsions. Am. J. Hosp. Pharm. 44, 2271–2280.

Sinko, P.J., 2006. Martin's Physical Pharmacy and Pharmaceutical Sciences, fifth ed. Lippincott Williams & Wilkins, Philadelphia, PA, 509–519.

Tripp, M.G., Menon, S.K., Mikrut, B.A., 1990. Stability of total nutrient admixtures in a dual-chamber flexible container. Am. J. Hosp. Pharm. 47, 2496–2503.

US Pharmacopeia 30/NF 25 Supplement 2, 2007. <729> Globule Size Distribution in Lipid Injectable Emulsions, US Pharmacopeial Convention, Rockville, MD, pp. 3968–3970.

Venkatesh, S., Li, J., Caldwell, K.D., Anderson, B.D., 1998. Compositional heterogeneity in parenteral lipid emulsions after sedimentation field flow fractionation. J. Pharm. Sci. 87, 859–866.

Washington, C., Chawla, A., Christy, N., Davis, S.S., 1989. The electrokinetic properties of phospholipid-stabilized fat emulsions. Int. J. Pharm. 54, 191–197.

Washington, C., 1990. The stability of intraveneous fat emulsions in total parenteral nutrition mixtures. Int. J. Pharm. 66, 1–21.

Washington, C., Ferguson, J.A., Irwin, S.E., 1993. Computational prediction of the stability of lipid emulsions in total nutrient admixtures. J. Pharm. Sci. 82, 808–812.

Washington, C., 1996. Stability of lipid emulsions for drug delivery. Adv. Drug Del. Rev. 20, 131–145.

Whateley, T.L., Steele, G., Urwin, J., Smail, G.A., 1984. Particle size of intralipid and mixed total parenteral nurtition mixtures. J. Clin. Hosp Pharm. 9, 113–126.

Zhang, X., Kirsch, L.E., 2003. An assessment of techniques for evaluating the physical stability of parenteral emulsions. PDA J. Pharm. Sci. Technol. 57, 300–315.